

Final Year Dissertation
Universitat Pompeu Fabra

From Volatility to Value at Risk: A Comparative Analysis Using Jump, SABR, and Rough Volatility Models

Ferran García Rovira - Bachelor's Degree in Economics
Arnau Reig Caballeria - Bachelor's Degree in Economics
Miquel Muñoz García-Ramos - Bachelor's Degree in Economics

Tutor: Elisa Alòs Alcalde

Academic Year: 2024-2025



Acknowledgement

We would like to express our sincere gratitude to:

- Our supervisor, Prof. Elisa Alòs, for her guidance, expertise, and encouragement throughout the development of this thesis.
- Our families, for their unconditional support, patience, and motivation during our studies.
- Our fellow classmates and friends, for the discussions, feedback, and shared moments that enriched this experience.

Abstract

Volatility plays a central role in both risk management and financial modeling. This thesis investigates how different volatility modeling approaches influence the computation of Value at Risk (VaR), a widely used metric for quantifying downside risk. We compare four models for estimating volatility: Black Scholes, Jump Diffusion models (Merton and Kou), Rough Volatility models based on fractional Brownian motion, and the SABR stochastic volatility model. Each volatility estimate is integrated into a Monte Carlo simulation framework based on the Black-Scholes model to compute one-day VaR at the 95% and 99% confidence levels. A sensitivity analysis is also conducted to assess the robustness of each model with respect to key calibration parameters.

Using historical data from the S&P 500 index (2006–2025), we simulate 30,000 price paths for each model and compute the corresponding VaR values. Our results show that jump models produce VaR estimates similar to those obtained using Black Scholes, though they differ substantially in kurtosis and tail shape. Jump Diffusion models generate more extreme outcomes and higher kurtosis, indicating a stronger representation of tail risk. In contrast, the SABR and Rough Volatility models yield lower VaR estimates and more concentrated return distributions across calibrations, suggesting they may understate extreme losses under typical parameter settings. These findings indicate that, depending on the calibration and market context, both Jump Diffusion and Black Scholes models can provide conservative VaR estimates, while models with smoother volatility dynamics may offer a different risk profile.

Keywords: Volatility modeling; Value at Risk; Black Scholes; Jump Diffusion; Rough Volatility

Contents

List of Figures

List of Tables

| | | |
|----------|--|----------|
| 1 | Introduction | 1 |
| 2 | Theoretical Framework | 3 |
| 2.1 | Risk measurement and the concept of VaR | 3 |
| 2.2 | The Black-Scholes Model as Pricing Framework | 5 |
| 2.3 | Volatility in the Black-Scholes context | 5 |
| 2.4 | Jump Diffusion Models (Merton and Kou) | 6 |
| 2.5 | SABR Model (Stochastic Alpha Beta Rho Model) | 6 |
| 2.6 | Fractional/Rough Volatility Models (Rough Bergomi) | 7 |
| 2.7 | From volatility estimation to VaR computation | 8 |
| 3 | Methodology | 9 |
| 3.1 | General workflow: from volatility to VaR | 9 |
| 3.2 | Estimation of volatility via different models | 10 |
| 3.2.1 | Black-Scholes (benchmark) | 10 |
| 3.2.2 | Jump Diffusion | 10 |
| 3.2.3 | SABR Stochastic Volatility Model | 11 |
| 3.2.4 | Rough Volatility | 12 |
| 3.3 | Pricing via Black-Scholes using estimated volatilities | 12 |
| 3.4 | VaR calculation based on simulated prices | 14 |

| | | |
|-----------------------------------|--|------------|
| 3.5 | Evaluation criteria: consistency and sensitivity | 14 |
| 4 | Empirical Application and Results | 15 |
| 4.1 | Dataset description and preprocessing | 15 |
| 4.2 | Implementation of volatility estimators | 16 |
| 4.3 | Price simulation using Black-Scholes | 16 |
| 4.4 | VaR results by volatility method | 17 |
| 4.5 | Comparative analysis and robustness checks | 18 |
| 5 | Discussion | 20 |
| 5.1 | Interpretation of differences | 20 |
| 5.2 | Model limitations and robustness | 21 |
| 6 | Conclusions | 23 |
| 6.1 | Summary of findings | 23 |
| 6.2 | Practical interpretation | 24 |
| 6.3 | Future research directions | 24 |
| Bibliography | | i |
| A GitHub Repository | | iii |
| B Figures | | iv |
| C Tables | | xv |
| D Mathematical Derivations | | xx |

List of Figures

| | | |
|----|---|-----|
| 1 | Realized volatility of the S&P 500 index computed over a rolling window of 20 days (2006–2024). | 1 |
| 2 | Realized volatility of the S&P 500 index computed over rolling windows of 5, 20, 60, 120, and 250 days (2006–2024). | iv |
| 3 | Histogram of daily log returns of the S&P 500 index from 2006 to 2024, compared with the fitted normal distribution. | v |
| 4 | Simulated 1-day returns generated using Black-Scholes model calibrated on historical S&P 500 data. | v |
| 5 | Simulated 1-day returns based on the Merton jump-diffusion model calibrated on historical S&P 500 data. | v |
| 6 | Simulated 1-day returns based on the Kou jump-diffusion model calibrated on historical S&P 500 data. | vi |
| 7 | Simulated 1-day returns based on the SABR model calibrated to S&P 500 data. | vi |
| 8 | Simulated 1-day returns based on the rough volatility model calibrated to S&P 500 data. | vi |
| 9 | Monte Carlo simulation of 1-day price paths based on Black-Scholes model calibrated to the S&P 500 index. | vii |
| 10 | Monte Carlo simulation of 1-day price paths based on the Merton Jump-Diffusion model calibrated to the S&P 500 index. | vii |
| 11 | Monte Carlo simulation of 1-day price paths based on the Kou Jump-Diffusion model calibrated to the S&P 500 index. | vii |

| | | |
|----|--|------|
| 12 | Monte Carlo simulation of 1-day price paths based on the SABR model calibrated to the S&P 500 index. | viii |
| 13 | Monte Carlo simulation of 1-day price paths based on the rough volatility model calibrated to the S&P 500 index. | viii |
| 14 | Histogram of 1-day returns simulated using the Black-Scholes model. | viii |
| 15 | Histogram of 1-day returns simulated using the Merton jump-diffusion model. | ix |
| 16 | Histogram of 1-day returns simulated using the Kou jump-diffusion model. | ix |
| 17 | Histogram of 1-day returns simulated using the SABR (Stochastic Alpha Beta Rho) model. | ix |
| 18 | Histogram of 1-day returns simulated using the rough volatility model. . | x |
| 19 | Detected jumps in daily log returns of the S&P 500 index from 2006 to 2024. | x |
| 20 | Comparison of simulated 1-day return distributions across models. | x |
| 21 | Zoom on the left tail of the simulated 1-day return distributions across models. | xi |
| 22 | Sensitivity of 1-day Value at Risk (VaR) at the 95% and 99% confidence levels to the length of the rolling volatility window in the Black-Scholes model. | xi |
| 23 | Sensitivity of 1-day Value at Risk (VaR) at the 95% and 99% confidence levels to the jump detection threshold in the Merton jump-diffusion model. | xi |
| 24 | Sensitivity of 1-day Value at Risk (VaR) at the 95% and 99% confidence levels to the jump detection threshold in the Kou jump-diffusion model. | xii |

| | | |
|----|---|------|
| 25 | Sensitivity of 1-day Value at Risk (VaR) at the 95% and 99% confidence levels to the volatility estimation window under the SABR log-normal model. | xii |
| 26 | Sensitivity of 1-day Value at Risk (VaR) at the 95% and 99% confidence levels to the volatility estimation window under the rough volatility model. | xii |
| 27 | Sensitivity of estimated jump parameters in the Merton model to the detection threshold. | xiii |
| 28 | Sensitivity of estimated jump parameters in the Kou model to the detection threshold. | xiii |
| 29 | Sensitivity of SABR model parameters to the volatility estimation window. | xiii |
| 30 | Sensitivity of rough volatility model parameters to the volatility estimation window. | xiv |

List of Tables

| | | |
|----|---|-------|
| 1 | S&P500 data 2006-2025 | 15 |
| 2 | Estimated parameters and simulated 1-day Value at Risk using Black-Scholes. | xv |
| 3 | Estimated parameters and simulated 1-day VaR using the Merton Jump Diffusion model. | xv |
| 4 | Estimated parameters and simulated 1-day VaR using the Kou Jump Diffusion model. | xvi |
| 5 | Estimated parameters and simulated 1-day VaR using the SABR model. | xvi |
| 6 | Estimated parameters and simulated 1-day VaR using the Rough Volatility model. | xvi |
| 7 | Comparison of 1-day VaR (95% and 99%) and kurtosis across different volatility models. | xvii |
| 8 | Sensitivity analysis of the parametric volatility model to the rolling window size used for realized volatility estimation. | xvii |
| 9 | Sensitivity analysis of the Merton Jump Diffusion model to jump detection thresholds. | xvii |
| 10 | Sensitivity analysis of the Kou Jump Diffusion model to the threshold used for jump detection. | xviii |
| 11 | Sensitivity analysis of the SABR model to the window size used for volatility estimation. | xviii |
| 12 | Sensitivity analysis of the Rough Volatility model to the window size used for volatility estimation. | xviii |

| | | |
|----|--|-----|
| 13 | Sensitivity analysis across all volatility models with varying calibration inputs. | xix |
|----|--|-----|

Chapter 1

Introduction

Volatility is a cornerstone of financial modeling and risk management, capturing the uncertainty inherent in asset prices. Its accurate estimation is crucial for derivative pricing, portfolio optimization, and regulatory compliance. However, conventional models—such as those assuming constant volatility or relying solely on historical data—often fail to capture key empirical features observed in financial markets, including sudden price jumps, volatility smiles, and persistent volatility clustering. The 2008 financial crisis exposed the fragility of standard risk models and reinforced the need for more realistic frameworks that can better anticipate and quantify extreme events.

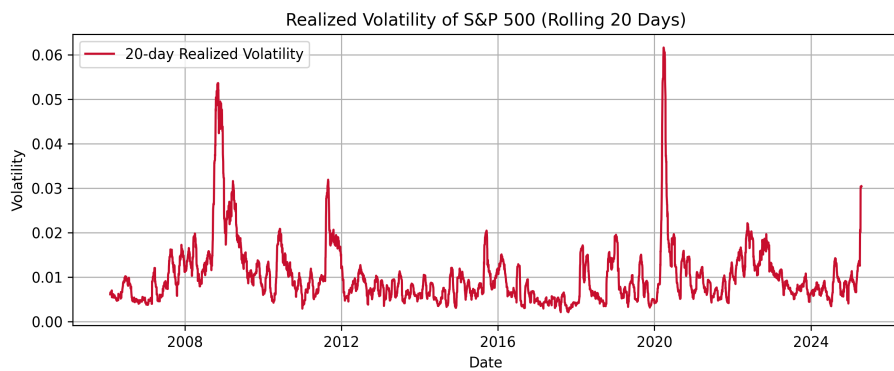


Figure 1: Realized volatility of the S&P 500 index computed over a rolling window of 20 days (2006–2024).

In this context, Value at Risk (VaR) remains one of the most widely adopted risk

metrics, yet its reliability depends heavily on the quality of the underlying volatility estimates. In recent years, several advanced models have been proposed to address the shortcomings of traditional approaches. Among these, jump diffusion, SABR (Stochastic Alpha Beta Rho) and rough volatility models, stand out as promising alternatives. Each captures distinct market phenomena: jump diffusion models account for abrupt price movements, SABR is particularly effective in modeling implied volatility surfaces and rough volatility models incorporate long-memory dynamics and irregular paths.

This thesis investigates how different volatility modeling approaches affect the computation of VaR. Specifically, it compares four methods: classical Black-Scholes (as a benchmark), Jump Diffusion models, the SABR Model and Rough Volatility models. The objective is to assess their relative effectiveness in estimating volatility and, consequently, in producing reliable VaR figures. The study aims to identify the trade-offs involved in each method, balancing theoretical rigor with empirical performance and practical feasibility.

The analysis proceeds in two stages. First, the theoretical foundations of each model are examined, focusing on their assumptions, mathematical structure, and relevance in financial literature. Second, the models are implemented in Python using real market data. Each estimated volatility series is input into the Black-Scholes framework (or the relevant pricing mechanism in the case of SABR) to simulate price paths, from which VaR is computed. The models are evaluated based on their predictive consistency and their sensitivity to changes in model parameters.

Chapter 2 presents the theoretical framework, including an overview of VaR, the Black-Scholes model, and the selected volatility models. Chapter 3 details the methodological workflow, from volatility estimation to VaR computation. Chapter 4 contains the empirical analysis and results. Chapter 5 discusses key insights and limitations, and Chapter 6 concludes with a summary and directions for future research. Technical appendices provide code, derivations, and supplementary material.

Chapter 2

Theoretical Framework

Understanding how volatility modeling affects Value at Risk (VaR) estimation is central to this thesis. While the Black-Scholes framework provides a tractable and widely accepted setting for simulating asset prices, the treatment of volatility within this framework critically shapes the distribution of returns and, consequently, the estimation of risk. This chapter lays out the theoretical basis of the models employed in this study. Beginning with the concept of VaR, it proceeds through the classical Black-Scholes model and its limitations, then presents alternative volatility modeling approaches: jump diffusions, SABR, and rough volatility models. Each is evaluated in terms of its implications for risk estimation.

2.1 Risk measurement and the concept of VaR

Quantifying potential losses in financial portfolios/securities is a fundamental objective in risk management. Institutions such as banks, asset managers, and regulators rely on robust metrics to assess exposure under both normal and stressed market conditions. Among various measures, Value at Risk (VaR) has become a standard due to its intuitive interpretation and regulatory endorsement (e.g., Basel II and III) (Jorion, 2007). VaR summarizes the potential loss of a portfolio/security over a specified time horizon at a given confidence level.

Formally, let ΔV denote the change in portfolio value over the horizon of interest. The Value at Risk at confidence level $\alpha \in (0, 1)$ is defined as the smallest value x such that the probability of a loss exceeding x does not exceed $1 - \alpha$:

$$P(\Delta V < VaR_\alpha) = \alpha$$

For example, a one-day 99% VaR of 1 million indicates that there is only a 1% chance that losses will exceed 1 million in a single day.

The three main methods to estimate VaR are: Historical Simulation, Delta-Normal, and Monte Carlo. All rely on recent historical data and differ in their assumptions:

- **Historical Simulation** recalculates portfolio returns using past x days of data and takes the 1st or 5th percentile as the VaR.
- **Delta-Normal** assumes normally distributed returns, estimates the variance-covariance matrix, and computes VaR analytically.
- **Monte Carlo** simulates many future scenarios using stochastic models to estimate the distribution of returns and derive the VaR.

These methods are described in (Jorion, 2007).

In this thesis, we adopt the Monte Carlo approach. Asset prices will be simulated using the Black-Scholes framework, with different specifications for the volatility input σ_t . This enables a controlled comparison of how volatility modeling affects the resulting VaR estimates.

2.2 The Black-Scholes Model as Pricing Framework

The Black-Scholes model (Black & Scholes, 1973) [?]emains a bedrock of modern financial theory. It assumes that asset prices follow geometric Brownian motion:

$$dS_t = \mu S_t dt + \sigma S_t dW_t$$

where μ is the drift, σ is constant volatility, and W_t is standard Brownian motion.

From this specification, the well-known Black-Scholes option pricing formula is derived. Though based on simplifying assumptions (e.g., frictionless markets, no transaction costs, continuous trading), the model offers an analytically tractable starting point.

In this thesis, the Black-Scholes framework is used as the common structure for all simulations. The core asset price dynamics remain the same across scenarios. The only variable component is the modeling of σ_t , allowing us to isolate the impact of volatility modeling on risk estimation.

2.3 Volatility in the Black-Scholes context

Although the Black-Scholes model assumes constant volatility, empirical data contradict this assumption. Market volatility is time-varying and exhibits features such as clustering, leverage effects, and fat tails (Cont, 2001).

In practice, volatility is often inferred from option prices as implied volatility. Observed volatility smiles and skews suggest that constant volatility fails to capture real market dynamics. Moreover, volatility's term structure is dynamic and frequently mean-reverting.

These limitations motivate the use of alternative volatility models. This thesis examines three such approaches: jump diffusions, SABR and rough volatility models. Each model is integrated into the Black-Scholes price simulation by varying only the volatility process.

2.4 Jump Diffusion Models (Merton and Kou)

Market prices can experience sudden jumps due to events like earnings announcements or geopolitical news. These jumps introduce skewness and excess kurtosis into return distributions.

Merton (1976) introduced a jump diffusion model:

$$dS_t = (\mu - \lambda k) S_t dt + \sigma S_t dW_t + S_t \left(\prod_{j=1}^{dN_t} Y_t - 1 \right)$$

where N_t is a Poisson process and Y_t the jump size. (To see an exhaustive mathematical derivation, consult Appendix D).

Kou (2002) proposed a double-exponential distribution for $\log(Y_t)$, allowing for asymmetric jumps. This model better captures volatility skews and is analytically tractable. The jump size density is given by:

$$f_J(x) = p \eta_1 e^{-\eta_1 x} \mathbf{1}_{x \geq 0} + (1 - p) \eta_2 e^{\eta_2 x} \mathbf{1}_{x < 0}$$

where $p \in (0, 1)$ is the probability of an upward jump, and $\eta_1, \eta_2 > 0$ are the decay parameters for upward and downward jumps, respectively.

In this study, we embed jumps into the volatility process while retaining the Black-Scholes structure for prices. This allows us to analyze how discontinuities affect VaR.

2.5 SABR Model (Stochastic Alpha Beta Rho Model)

The SABR model (Hagan et al., 2002) is widely used in interest rate and FX derivatives. It specifies the forward price F_t and volatility σ_t as:

$$\begin{cases} dF_t = \sigma_t F_t^\beta dW_t \\ d\sigma_t = \nu \sigma_t dZ_t \\ \text{with } \mathbb{E}[dW_t dZ_t] = \rho dt \end{cases}$$

In this thesis, we adapt the model to simulate spot prices rather than forward prices, fixing $\beta = 1$ to ensure log-normality. This is appropriate for equity indices like the S&P 500, where spot and forward prices are nearly equivalent in low-rate, short-horizon environments. The volatility process is driven by standard Brownian motion, which implies a temporal roughness corresponding to a Hurst parameter $H = 1/2$. Parameters are calibrated from historical data.

2.6 Fractional/Rough Volatility Models (Rough Bergomi)

Traditional models like the ones we have seen up to now assume that volatility follows smooth, continuous paths—typically modeled as diffusions driven by Brownian motion. However, empirical studies have revealed that actual market volatility exhibits roughness, characterized by irregular, jagged paths with low Hölder continuity (Gatheral et al. 2018).

In Alòs, León, and Vives (2007), it was shown using Malliavin calculus that one can dispense with the Markovian, semimartingale assumption on σ_t altogether and still recover the empirically observed short-time skew of implied volatilities. In particular, their framework admits volatility processes with fractional dynamics, whose rougher trajectories naturally generate the steep, term-structure-dependent skews seen in the market.

Building on this insight, Gatheral, Jaisson, and Rosenbaum (2018) and Bayer, Friz, and Gatheral (2016) proposed a concrete “rough” stochastic volatility model. High-frequency data reveal that log-volatility behaves almost like a fractional Brownian motion with Hurst exponent $H \approx 0.1$ —much “rougher” than standard Brownian motion at all relevant time scales. This empirical finding motivated a new class of models known as Rough Volatility models.

The rough Bergomi model (Bayer et al., 2016) formulates volatility as:

$$\sigma_t = \xi_0(t) \exp \left(\eta \int_0^t (t-s)^{H-1/2} dZ_s - \frac{1}{2} \eta^2 t^{2H} \right)$$

This leads to short-memory, heavy-tailed return distributions.

Simulating asset prices with rough volatility under the Black-Scholes framework allows us to assess the risk implications of this irregular behavior. This provides a third stochastic volatility model for VaR estimation, alongside jump and SABR approaches.

2.7 From volatility estimation to VaR computation

Each volatility model discussed above yields a different shape for the return distribution generated via simulation. These differences, though subtle in modeling, have major implications for the estimation of VaR:

All simulations retain the Black-Scholes price structure and differ only in the volatility process. For each model, we simulate many paths of asset prices, compute changes in portfolio value ΔV , and estimate VaR as the empirical quantile:

$$P(\Delta V < VaR_\alpha) = \alpha$$

This approach ensures a consistent comparison across models, helping identify whether more sophisticated volatility specifications lead to meaningfully improved risk assessments.

Chapter 3

Methodology

This section outlines the full methodological framework used to estimate Value at Risk (VaR) based on different volatility models. The process follows a structured pipeline: first, volatility is estimated using four different approaches; second, this volatility is used to price one-day-ahead asset values via a modified Black-Scholes model; finally, VaR is computed from the resulting distribution of simulated returns.

3.1 General workflow: from volatility to VaR

The goal of this chapter is to assess how different volatility modeling assumptions impact the resulting Value at Risk (VaR) estimates. The workflow comprises three main stages:

- **Volatility Estimation:** The daily volatility of the S&P 500 is estimated using four models:
 - Classical Black-Scholes
 - Jump Diffusion (Merton and Kou)
 - SABR Stochastic Volatility Model
 - Rough Volatility (fractional Brownian motion)

- **Pricing:** Using each estimated volatility model, the Black-Scholes pricing framework is adapted to simulate 30,000 possible one-day-ahead price paths starting from a normalized price.
- **VaR Calculation:** From the distribution of simulated returns, the 95% and 99% quantiles are computed to derive the 1-day VaR under each volatility specification.

The following sections explain each component in detail.

3.2 Estimation of volatility via different models

3.2.1 Black-Scholes (benchmark)

As a benchmark, we assume the Black-Scholes model with constant volatility. This volatility is estimated from historical data using the standard deviation of daily log returns over the selected sample period:

$$\sigma^{BS} = \sqrt{\frac{1}{n-1} \sum_{i=1}^n (r_i - \bar{r})^2}, \quad \text{where } r_i = \log\left(\frac{P_i}{P_{i-1}}\right)$$

This value of σ^{BS} is then treated as constant and used in the simulation of asset prices under the Black-Scholes framework.

3.2.2 Jump Diffusion

We implement two types of jump models: the classical Merton Jump Diffusion model, and the Double Exponential model proposed by Kou. In both cases, jumps are detected empirically from the log return series as extreme values beyond $\pm 2.5\sigma$.

- **Merton model:**

$$dS_t = \mu S_t dt + \sigma S_t dW_t + J_t S_t dN_t$$

where $dN_t \sim \text{Poisson}(\lambda)$ and $J_t \sim \mathcal{N}(\mu_J, \sigma_J^2)$.

- **Kou model:** Jumps follow a double exponential distribution:

$$f_J(x) = p\eta_1 e^{-\eta_1 x} \mathbf{1}_{x>0} + (1-p)\eta_2 e^{\eta_2 x} \mathbf{1}_{x<0}$$

with parameters p, η_1, η_2 estimated empirically from positive and negative jumps.

3.2.3 SABR Stochastic Volatility Model

The SABR (Stochastic Alpha Beta Rho) model, commonly used in interest rate markets, is adapted here to estimate stochastic volatility on spot price series. We assume log-normal dynamics ($\beta = 1$):

$$\begin{cases} dS_t = \sigma_t S_t^\beta dW_t \\ d\sigma_t = \nu \sigma_t dZ_t \\ \text{with } \mathbb{E}[dW_t dZ_t] = \rho dt \end{cases}$$

Parameters are calibrated as follows:

- ξ_0 : initial volatility, taken as the mean of a 20-day rolling window.
- ν : volatility of volatility, computed as the standard deviation of realized volatility.
- ρ : correlation between returns and volatility changes, estimated via Pearson correlation.

This model introduces correlated stochastic shocks to price and volatility, capturing leverage effects and forward-looking uncertainty.

3.2.4 Rough Volatility

Following Gatheral et al. (2018), we model volatility as a lognormal process driven by fractional Brownian motion (fBM):

$$\sigma_t = \xi_0 \exp \left(\nu W_t^H - \frac{1}{2} \nu^2 t^{2H} \right)$$

where:

- W_t^H is fractional Brownian motion (fBM) with Hurst exponent,
- ξ_0 is the initial volatility (mean of realized volatility),
- ν is the volatility of volatility (standard deviation of realized volatility),
- H is estimated from the volatility series via the `hurst` method.

In this setup, the volatility process is non-Markovian and rough, capturing empirical features of financial markets not present in classical models.

3.3 Pricing via Black-Scholes using estimated volatilities

Once the volatility has been estimated using the three models described above, we proceed to simulate future asset prices over a one-day horizon. To ensure comparability, we normalize the current price as $S_0 = 100$ and use a modified version of the Black-Scholes pricing equation to generate simulated prices:

$$S_T = S_0 \cdot \exp \left(\left(\mu - \frac{1}{2} \sigma^2 \right) T + \sigma \sqrt{T} Z \right)$$

where:

- μ is the annualized drift, calibrated from historical log returns,
- σ is the estimated volatility for each model,

- $Z \sim \mathcal{N}(0, 1)$ is a standard normal random variable,
- $T = 1/252$ represents one trading day.

In the case of jump models, an additional jump component J is added inside the exponential, reflecting the impact of rare, large price movements:

$$S_T^{\text{jump}} = S_0 \cdot \exp \left(\left(\mu - \frac{1}{2} \sigma^2 \right) T + \sigma \sqrt{T} Z + J \right)$$

In the SABR case, both the volatility path σ_t and its correlation with the asset price are simulated jointly. Euler discretization is used to propagate the coupled SDE system, capturing the co-evolution of price and volatility over the one-day horizon.

$$\begin{aligned} \sigma_{t+\Delta t} &= \sigma_t + \nu \sigma_t \sqrt{\Delta t} Z_1 \\ S_{t+\Delta t} &= S_t \cdot \exp \left(-\frac{1}{2} \sigma_t^2 \Delta t + \sigma_t \sqrt{\Delta t} Z_2 \right) \end{aligned}$$

with correlated Gaussian shocks $\text{Corr}(Z_1, Z_2) = \rho$.

For the rough volatility model, the volatility σ_t is simulated path-by-path from the rough stochastic volatility process, making the effective endogenous to each simulation.

$$\sigma_t = \xi_0(t) \cdot \exp \left(\eta \int_0^t (t-s)^{H-\frac{1}{2}} dZ_s - \frac{1}{2} \eta^2 t^{2H} \right)$$

The asset price is then simulated as:

$$S_T = S_0 \cdot \exp \left(-\frac{1}{2} \sigma_t^2 T + \sigma_t \sqrt{T} W \right)$$

In all cases, 30,000 price paths are simulated using the corresponding model parameters, forming the empirical distribution from which returns and VaR are subsequently derived.

3.4 VaR calculation based on simulated prices

With the distribution of one-day-ahead simulated prices $\left\{S_T^{(i)}\right\}_{i=1}^n$ obtained from each model, we calculate the corresponding distribution of returns as:

$$R^{(i)} = \frac{S_T^{(i)} - S_0}{S_0}$$

Then, the 1-day Value at Risk at a confidence level is defined as:

$$VaR_\alpha = -S_0 \cdot Quantile_{1-\alpha}(R)$$

For this study, we compute the VaR at the 95% and 99% levels ($\alpha = 0.95$ and $\alpha = 0.99$). The Monte Carlo procedure ensures that the shape of the return distribution reflects the properties of each volatility model, including fat tails and asymmetry.

3.5 Evaluation criteria: consistency and sensitivity

To assess the performance and robustness of each model, two evaluation criteria are applied to the resulting VaR estimates:

- **Internal Consistency:** We verify that the VaR estimates are coherent with the distributional properties of the underlying simulations. In particular, we examine whether models that introduce jumps, stochastic volatility, or roughness lead to heavier tails and higher VaR, as theoretically expected.
- **Sensitivity Analysis:** The sensitivity of VaR estimates to changes in model inputs (such as window size for volatility, or threshold for jump detection) is assessed. This helps to identify which models are more stable versus those that are more reactive to input variations.

These evaluation tools are crucial not only for comparing models on statistical grounds, but also for assessing their practical usefulness.

Chapter 4

Empirical Application and Results

4.1 Dataset description and preprocessing

The empirical analysis is based on historical price data for the S&P 500 index, retrieved using the `yfinance` Python package. The sample period spans from January 2006 to April 2025, covering a wide range of market conditions, including both tranquil and crisis episodes.

For each trading day, the dataset includes open, high, low, close, and volume prices.

| Date | Close | High | Low | Open | Volume |
|------------|-------------|-------------|-------------|-------------|------------|
| 2006-01-03 | 1268.800049 | 1270.219971 | 1245.739990 | 1248.290039 | 2554570000 |
| 2006-01-04 | 1273.459961 | 1275.369995 | 1267.739990 | 1268.800049 | 2515330000 |
| ... | ... | ... | ... | ... | ... |
| 2025-04-16 | 5275.700195 | 5367.240234 | 5220.790039 | 5335.750000 | 4607750000 |
| 2025-04-17 | 5282.700195 | 5328.310059 | 5255.580078 | 5305.450195 | 4714880000 |

Table 1: S&P500 data 2006-2025

From this raw data, the following variables were constructed:

- Logarithmic daily returns, defined as $r_t = \log(P_t/P_{t-1})$.
- Realized volatility, estimated as the rolling standard deviation of daily returns using windows of 5, 20, 60, 120, and 250 days.

Missing values resulting from non-trading days or rolling window truncation were dropped. The resulting cleaned dataset serves as the input for model calibration and Monte Carlo simulation. Figure 2 illustrates the behavior of realized volatility across multiple horizons, providing visual motivation for the need to explore alternative volatility models.

4.2 Implementation of volatility estimators

Each volatility model was calibrated using market data. For the classical Black-Scholes, volatility is estimated directly from historical returns. For the jump diffusion models, jumps were identified as returns exceeding a 2.5 standard deviation threshold. The estimated parameters for the Merton model are the jump frequency λ , average jump size μ_J , and jump standard deviation σ_J . For the Kou model, upward and downward jumps were separated, and exponential decay parameters η_1 and η_2 were estimated.

The SABR model, adapted to the context of spot price simulation, is calibrated using the correlation between log-returns and volatility innovations, producing a value for ρ . The rough volatility model uses the 20-day realized volatility to estimate the Hurst exponent H , mean volatility ξ_0 , and volatility of volatility ν . These parameters are inferred via the `fbm` and `hurst` Python libraries.

All models are calibrated from the same underlying dataset to allow consistent and fair comparison in the subsequent simulation and VaR analysis.

4.3 Price simulation using Black-Scholes

To isolate the effect of volatility modeling, all price paths are simulated using the Black-Scholes framework:

$$dS_t = \mu S_t dt + \sigma_t S_t dW_t$$

where the only difference across simulations lies in the modeling of σ_t .

For each model, 30,000 price paths were generated over a 1-day horizon, starting

from $S_0 = 100$. The simulated returns were computed as percentage changes from S_0 . The simulation results exhibit notable differences:

- The classical Black-Scholes model produces a near-Gaussian distribution (Table 2 and Figure 9).
- The Merton and Kou models introduce visible skewness and kurtosis through jump components (Tables 3 4 and Figures 10 11).
- The SABR and Rough Volatility models produce similar results, with symmetric distributions and thinner tails compared to those of the jump and historical models (Tables 5 6 and Figures 12 13).

These features are consistent with theoretical expectations in the case of jump models. However, the fact that the SABR and Rough Volatility models do not produce heavier tails may be influenced by factors such as the chosen data window, the characteristics of the input series, or the calibration of roughness and correlation parameters.

4.4 VaR results by volatility method

The Value at Risk (VaR) at 95% and 99% confidence levels was computed from the distribution of simulated returns. All VaR figures are reported on a one-day horizon. Table 7 (in the Appendix) summarizes the results.

The SABR and Rough Volatility models consistently produce the lowest VaR estimates, indicating lower perceived tail risk. In contrast, the jump models (Merton and Kou) generate higher VaR, particularly at the 99% level, reflecting their sensitivity to extreme events. The Black-Scholes model yields VaR estimates similar to those of the jump models, but clearly differs in kurtosis. This suggests that while the VaR values may be close, the jump models explicitly account for more extreme scenarios, which are not captured by the Black-Scholes.

Interestingly, although the Kou and Merton models exhibit higher kurtosis—capturing the presence of fat tails and extreme outcomes—their VaR estimates are not substantially higher than those of other models. This highlights a key insight: higher kurtosis does not necessarily imply greater Value at Risk. While kurtosis reflects the likelihood of extreme returns in the distribution, VaR focuses on a specific quantile, and the two measures do not always move in tandem. These findings caution against overinterpreting tail metrics when assessing risk through quantile-based measures like VaR.

4.5 Comparative analysis and robustness checks

The models were compared using graphical and statistical tools. Figures 20 and 21 included in the appendix display simulated return densities, overlaid to illustrate tail behavior (kurtosis in Table 7). Key observations include:

- Jump models display much heavier tails than the other approaches, with pronounced left skew and clear deviations from normality.
- The SABR and Rough Volatility models show narrower return distributions with thinner tails, indicating less extreme simulated outcomes.

Sensitivity analyses were conducted by varying two key calibration inputs: the jump detection threshold for Jump Diffusion models, and the volatility estimation window for the remaining ones. Changes in the jump threshold had minimal impact on the resulting VaR estimates, suggesting robustness in the jump-based models (Figures 23 and 24). In contrast, the volatility window had a significant effect. In the classical Black-Scholes, longer windows (e.g., 250 days) produced notably lower VaR values, while very short windows (e.g., 5 days) also underestimated risk (Figure 22). Both the SABR and Rough Volatility models showed increasing VaR estimates with longer volatility windows, highlighting their sensitivity to persistent volatility inputs (Figures 25 and 26).

These findings reinforce the importance of parameter selection in volatility modeling.

While jump models are relatively stable in terms of VaR, models relying on realized volatility estimates—such as classical Black-Scholes, SABR, and Rough—can yield markedly different results depending on the observation window used.

The full set of sensitivity analysis results is shown in Table 13 in the Appendix.

Chapter 5

Discussion

5.1 Interpretation of differences

This section interprets the differences in Value at Risk (VaR) estimates obtained from various volatility modeling approaches applied within the Black-Scholes framework: classical Black-Scholes, jump diffusion (Merton and Kou), SABR, and rough volatility models.

Jump diffusion models tend to produce VaR estimates similar to, or slightly higher than, those obtained using historical volatility. While the numerical differences in VaR are modest, jump models exhibit significantly higher kurtosis and visibly heavier tails, indicating their superior ability to capture extreme events and asymmetric tail risk (Table 7).

In contrast, SABR and rough volatility models yield consistently lower VaR estimates in this study, likely due to smoother volatility paths and thinner tails in the simulated return distributions. For example, the rough model—with a relatively high Hurst exponent (Table 6)—generates volatility paths that are less reactive in the short term, resulting in more concentrated return distributions. The model produces a return distribution that is concentrated and symmetric, with relatively thin tails—closely resembling those of the SABR model (Table 5).

These differences underscore that similar VaR figures can arise from distributions with very different shapes, and that kurtosis and VaR—while both related to tail risk—do not always align. This reinforces the need for multi-dimensional risk metrics.

5.2 Model limitations and robustness

Each model presents distinct trade-offs. The classical Black-Scholes model, while simple and intuitive, is highly sensitive to the chosen rolling window (Table 8). Short windows (e.g., 20 days) can react strongly to recent volatility shocks—such as the significant increase in market volatility observed following the announcement of new trade tariffs by the Trump administration—leading to elevated VaR estimates despite moderate kurtosis. In contrast, longer windows smooth out recent volatility spikes and may underestimate short-term risk. This responsiveness can be a strength for detecting turbulence, but it also introduces instability in risk forecasts.

Jump-diffusion models explicitly capture tail risk through discontinuities in returns. While their calibration relies on a threshold-based method to detect jumps, the sensitivity analysis shows that their resulting VaR estimates remain relatively stable across different detection thresholds (Tables 9 and 10). This robustness, along with the ability to reflect skewness and fat tails (i.e., leptokurtosis) (Table 13), makes them particularly suitable for modeling extreme scenarios—though it also introduces challenges in calibration and interpretation.

SABR and Rough volatility models produce VaR estimates that are strongly influenced by the length of the volatility input window (Tables 11 and 12). As the window increases, both models yield progressively higher VaR values—though still below those obtained with jump models. Their simulated return distributions consistently exhibit low kurtosis and high concentration, suggesting that, despite incorporating stochastic features, these models tend to underrepresent short-term tail risk under typical calibrations (Table 13).

Overall, no single model dominates across all dimensions. Jump-diffusion models

consistently produce higher kurtosis and more extreme simulated returns, with relatively stable VaR estimates across calibration thresholds. However, the comparison with realized volatility is not straightforward. Depending on the chosen window, the historical model can also produce elevated VaR estimates, especially when recent market movements have triggered substantial increases in volatility. SABR and Rough volatility models, while sensitive to the input window, continue to yield lower VaR values across calibrations. Although rough volatility shows an upward trend in VaR with larger windows, its estimates remain below those of the jump and historical models in the data sample studied. These results reflect the distinct risk profiles each approach captures and suggest that model performance depends strongly on market conditions and input choices.

Chapter 6

Conclusions

6.1 Summary of findings

This thesis aimed to analyze how the estimation of volatility impacts the computation of Value at Risk (VaR) under the Black-Scholes framework, by comparing four alternative approaches: the classical Black Scholes, jump-diffusion models (Merton and Kou), the SABR stochastic volatility model, and rough volatility models based on fractional Brownian motion. The key findings are:

- Volatility modeling has a significant impact on VaR estimates. Jump-diffusion models and historical volatility yield similar VaR levels under certain configurations, but differ substantially in kurtosis and tail structure.
- The Kou model outperforms Merton in capturing asymmetric jumps. This leads to slightly higher VaR estimates and a more accurate reflection of left-tail risk.
- SABR and Rough volatility models consistently produce lower VaR estimates across calibrations. While their values increase with longer input windows, they remain below those of jump and historical models in the sample studied.
- Despite incorporating more complex volatility dynamics, the return distributions generated by SABR and rough models exhibit low kurtosis and strong

concentration, indicating limited ability to reflect short-term tail risk.

- The historical volatility model is sensitive to the selected rolling window. Short windows, in particular, can produce elevated VaR estimates when recent market volatility is high.

6.2 Practical interpretation

The empirical results show that no single model is superior in all respects. Jump-diffusion models are effective at capturing extreme return behavior and are relatively robust to changes in calibration thresholds. However, depending on recent market conditions, historical volatility with short rolling windows can also produce conservative risk estimates. SABR and Rough models tend to produce lower VaR estimates, with outcomes that vary depending on the length of the volatility input window. Their return distributions remain concentrated and low in kurtosis, which may limit their ability to reflect tail risk. These contrasts illustrate the importance of understanding the specific assumptions and sensitivities embedded in each volatility model when interpreting VaR outputs.

6.3 Future research directions

Several avenues for future work emerge from this research:

- Model calibration and estimation. Future work could investigate more efficient or robust methods for calibrating jump and rough volatility models on real-time data, especially in high-frequency environments.
- Extension to other derivative pricing models. This study focused on Black-Scholes; extending the analysis to stochastic volatility frameworks like Heston or multifactor SABR could yield richer insights.
- Stress testing applications. Applying these models in macroeconomic or geopolitical stress testing scenarios could assess their robustness and predictive power under extreme conditions.

- Portfolio-level VaR. While this study analyzed a single asset, extending the framework to a multi-asset portfolio with correlated risk factors would bring the analysis closer to real-world portfolio management.
- Use of Machine Learning techniques. Hybrid approaches that combine traditional financial models with machine learning could be explored to improve volatility forecasting and VaR accuracy.
- Regulatory implications. Further research could also explore how these advanced models align with Basel III/IV regulations and the potential for regulatory acceptance of non-linear VaR estimators.

Bibliography

- [1] Alòs, E., León, J. A. & Vives, J. On the short-time behavior of the implied volatility for jump-diffusion models with stochastic volatility. *Finance and Stochastics* **11**, 571–589 (2007).
- [2] Alòs, E. & León, J. A. An intuitive introduction to fractional and rough volatilities. *Mathematics* **9**, 994 (2021).
- [3] Duffie, D. & Pan, J. An overview of value at risk (1997). Preliminary Draft, January 21, 1997.
- [4] Artzner, P., Delbaen, F., Eber, J. & Heath, D. Coherent measures of risk. *Mathematical Finance* **9**, 203–228 (1999).
- [5] Jorion, P. *Value at Risk: The New Benchmark for Managing Financial Risk* (McGraw-Hill, 2007), 3rd edn.
- [6] Black, F. & Scholes, M. The pricing of options and corporate liabilities. *Journal of Political Economy* **81**, 637–654 (1973).
- [7] Cont, R. Empirical properties of asset returns: stylized facts and statistical issues. *Quantitative Finance* **1**, 223–236 (2001).
- [8] Bollerslev, T. Generalized autoregressive conditional heteroskedasticity. *Journal of Econometrics* **31**, 307–327 (1986).
- [9] Engle, R. Autoregressive conditional heteroscedasticity with estimates of the variance of united kingdom inflation. *Econometrica* **50**, 987–1007 (1982).

- [10] Hull, J. & White, A. The pricing of options on assets with stochastic volatilities. *Journal of Finance* **42**, 281–300 (1987).
- [11] Hull, J. & White, A. A closed-form solution for options with stochastic volatility with applications to bond and currency options. *Review of Financial Studies* **6**, 327–343 (1993).
- [12] Merton, R. Option pricing when underlying stock returns are discontinuous. *Journal of Financial Economics* **3**, 125–144 (1976).
- [13] Merton, R. A jump-diffusion model for option pricing. *Management Science* **48**, 1086–1101 (2002).
- [14] Eraker, B., Johannes, M. & Polson, N. The impact of jumps in volatility and returns. *Journal of Finance* **58**, 1269–1300 (2003).
- [15] Hagan, P., Kumar, D., Lesniewski, A. & Woodward, D. Managing smile risk. *Wilmott Magazine* **Sep**, 84–108 (2002).
- [16] Antonov, A., Konikov, M. & Spector, M. *Modern SABR Analytics: Formulas and Insights for Quants, Former Physicists and Mathematicians* (Springer, Cham, 2019).
- [17] Bayer, C., Friz, P. & Gatheral, J. Pricing under rough volatility. *Quantitative Finance* **16**, 887–904 (2016).
- [18] Bennedsen, M., Lunde, A. & Pakkanen, M. Hybrid semiparametric modeling of volatility: Getting the roughness right. *Journal of Econometrics* **207**, 90–113 (2017).
- [19] Gatheral, J., Jaisson, T. & Rosenbaum, M. Volatility is rough. *Quantitative Finance* **18**, 933–949 (2018).

Appendix A

GitHub Repository

All the code used for the simulations, data processing, and Value at Risk (VaR) computations presented in this thesis is available at the following GitHub repository:

<https://github.com/ferrangarciarovira/VaR-Volatility-Models>

This repository contains the full set of scripts and resources used to implement the models discussed in the empirical analysis, including data handling, Monte Carlo simulations, and plotting routines.

Appendix B

Figures

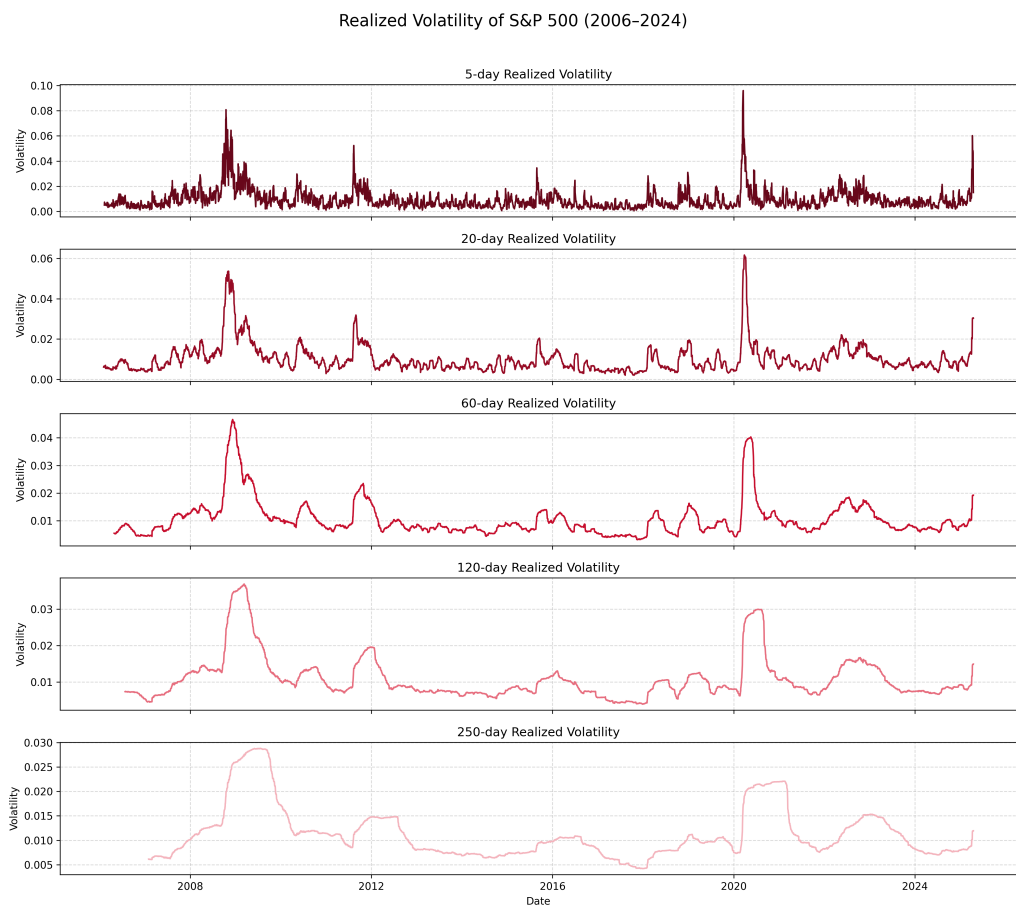


Figure 2: Realized volatility of the S&P 500 index computed over rolling windows of 5, 20, 60, 120, and 250 days (2006–2024).

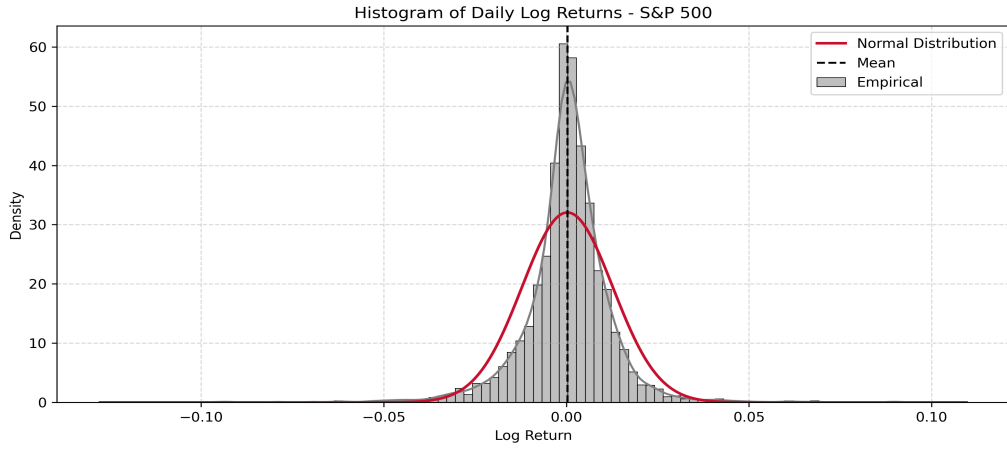


Figure 3: Histogram of daily log returns of the S&P 500 index from 2006 to 2024, compared with the fitted normal distribution.

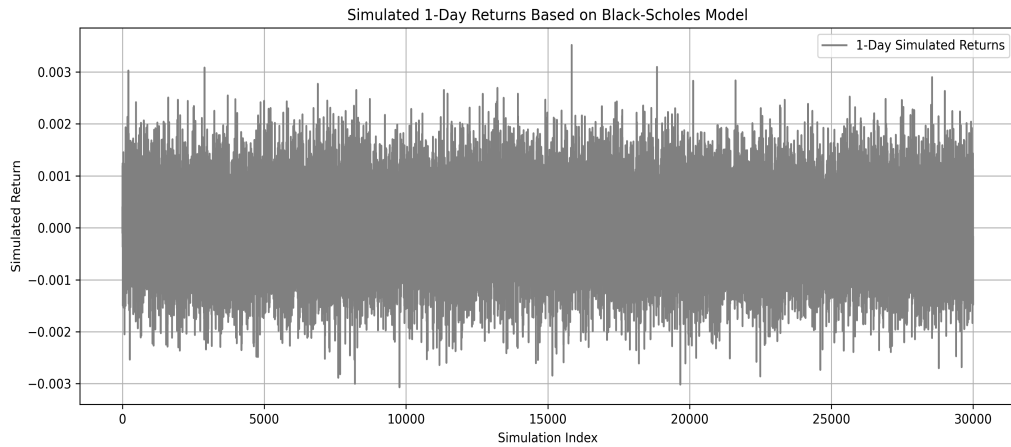


Figure 4: Simulated 1-day returns generated using Black-Scholes model calibrated on historical S&P 500 data.

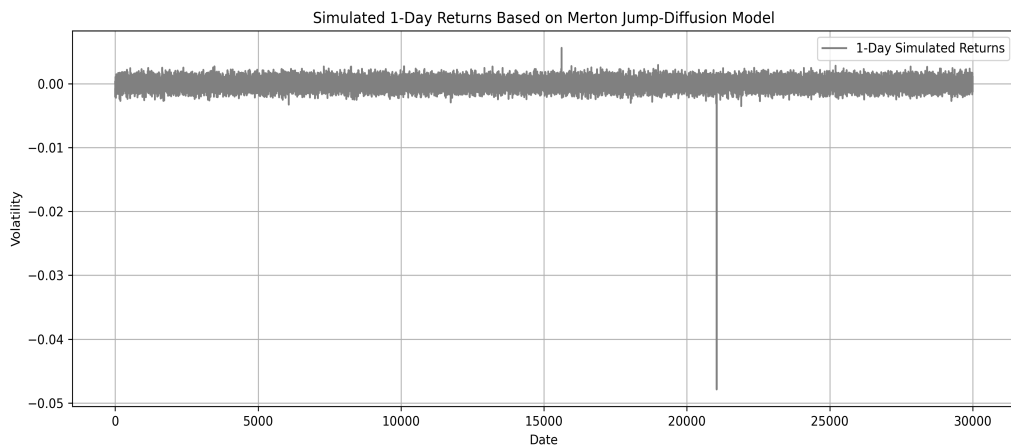


Figure 5: Simulated 1-day returns based on the Merton jump-diffusion model calibrated on historical S&P 500 data.

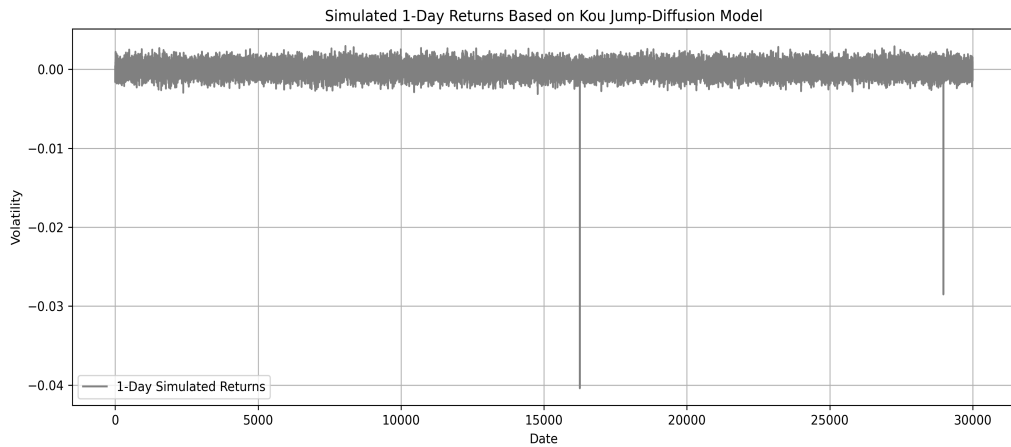


Figure 6: Simulated 1-day returns based on the Kou jump-diffusion model calibrated on historical S&P 500 data.

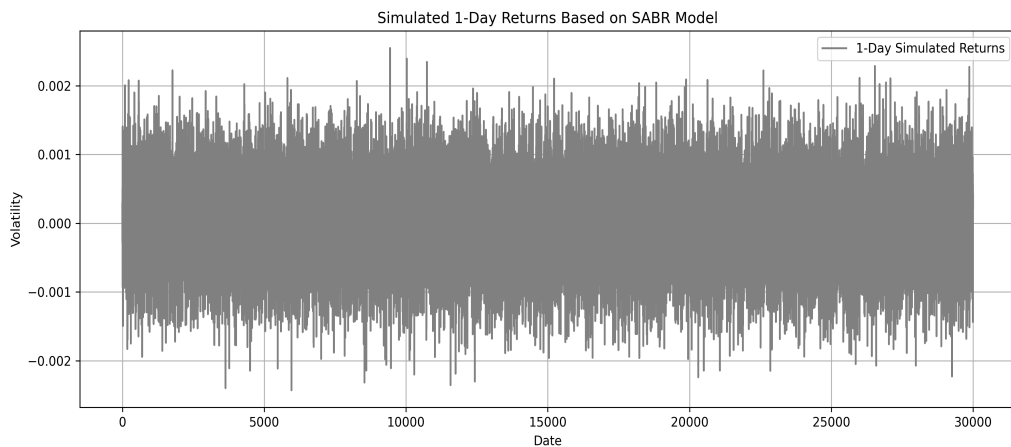


Figure 7: Simulated 1-day returns based on the SABR model calibrated to S&P 500 data.

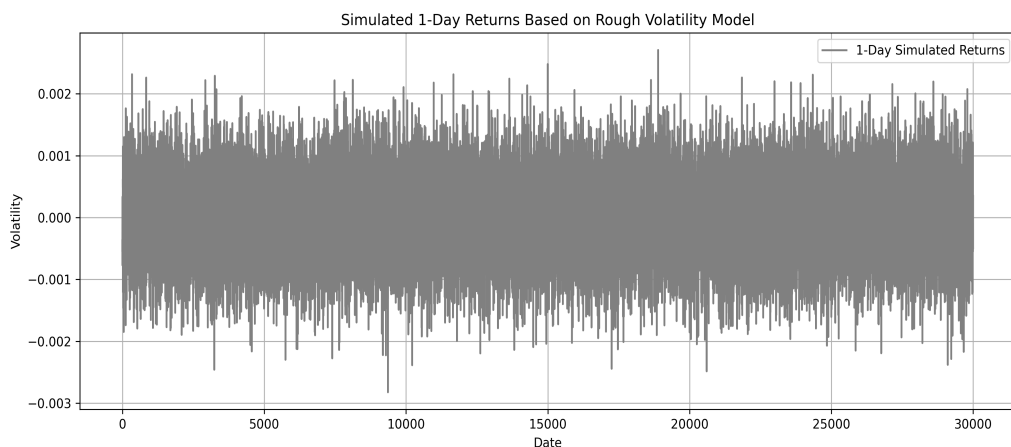


Figure 8: Simulated 1-day returns based on the rough volatility model calibrated to S&P 500 data.

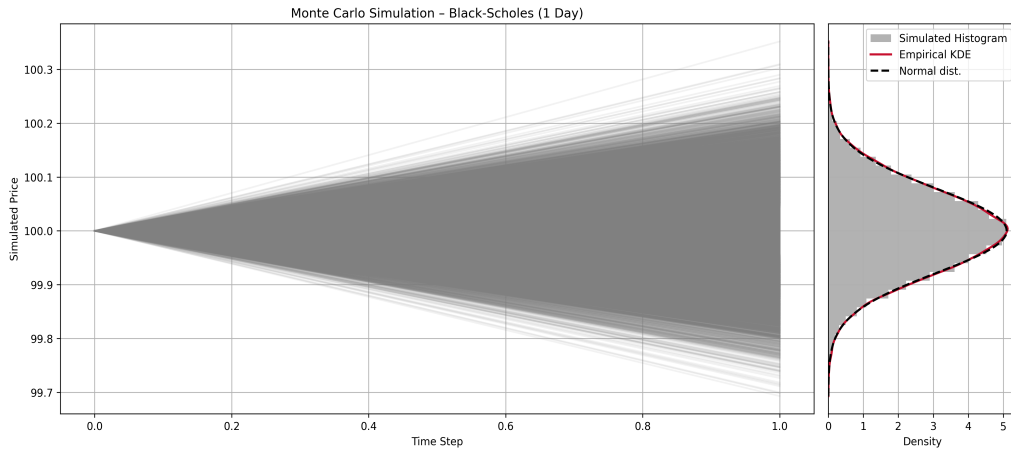


Figure 9: Monte Carlo simulation of 1-day price paths based on Black-Scholes model calibrated to the S&P 500 index.

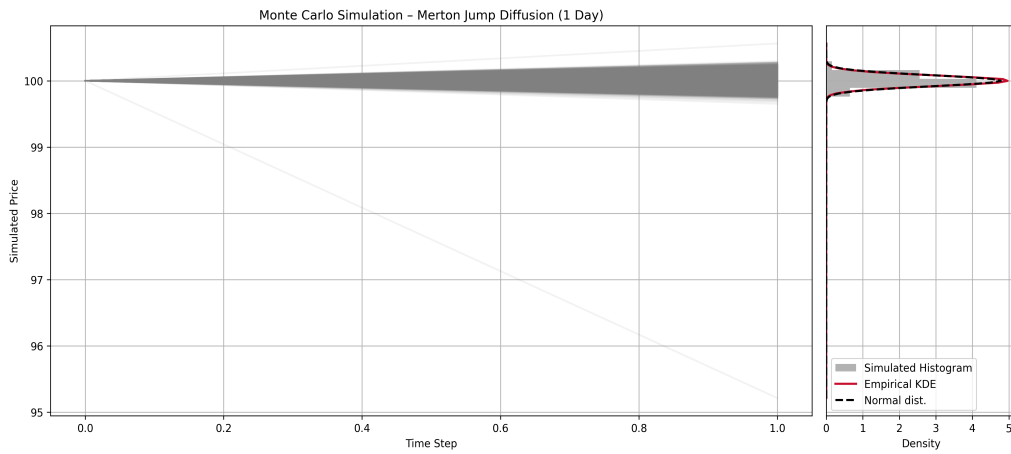


Figure 10: Monte Carlo simulation of 1-day price paths based on the Merton Jump-Diffusion model calibrated to the S&P 500 index.

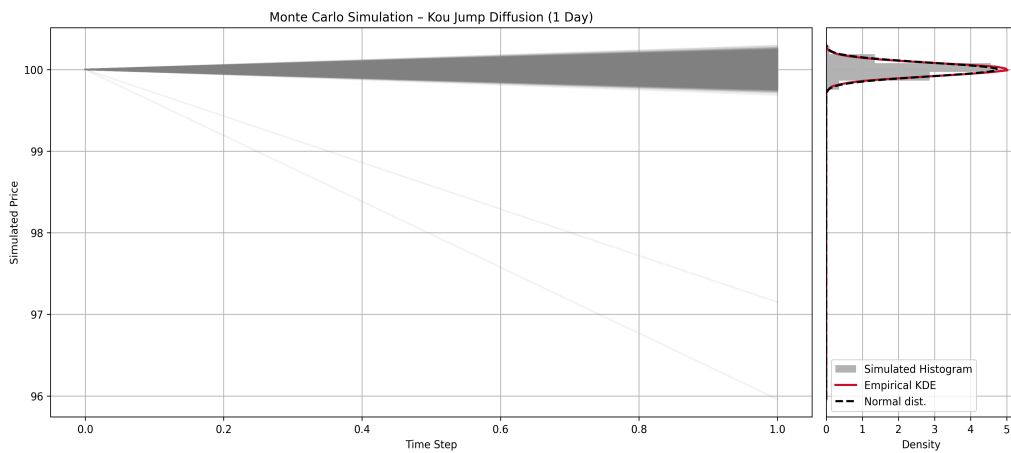


Figure 11: Monte Carlo simulation of 1-day price paths based on the Kou Jump-Diffusion model calibrated to the S&P 500 index.

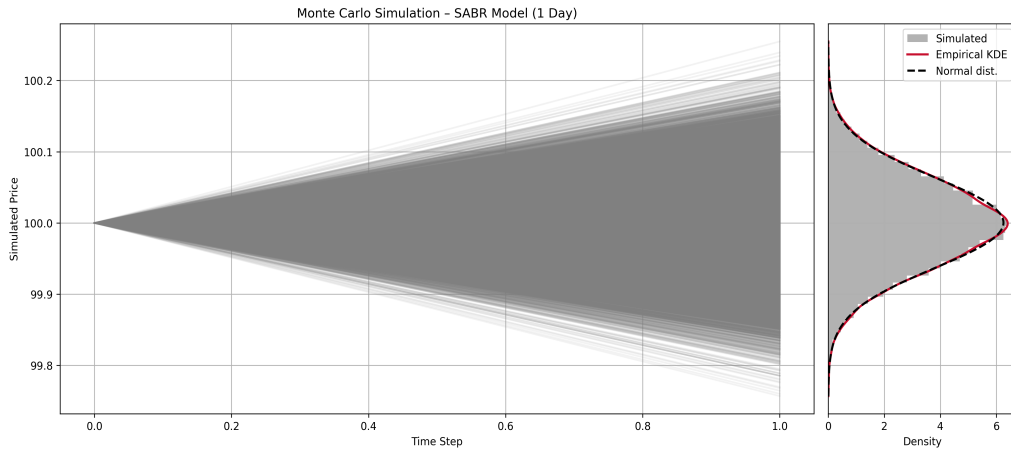


Figure 12: Monte Carlo simulation of 1-day price paths based on the SABR model calibrated to the S&P 500 index.

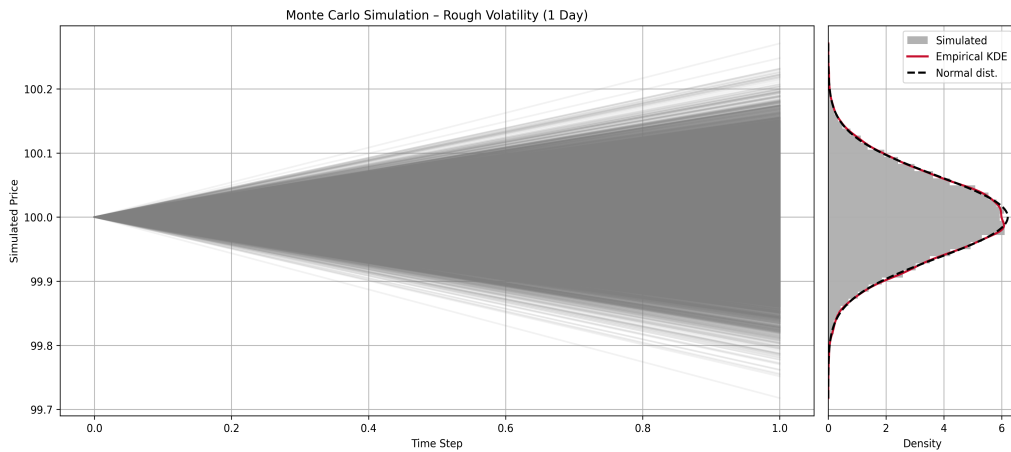


Figure 13: Monte Carlo simulation of 1-day price paths based on the rough volatility model calibrated to the S&P 500 index.

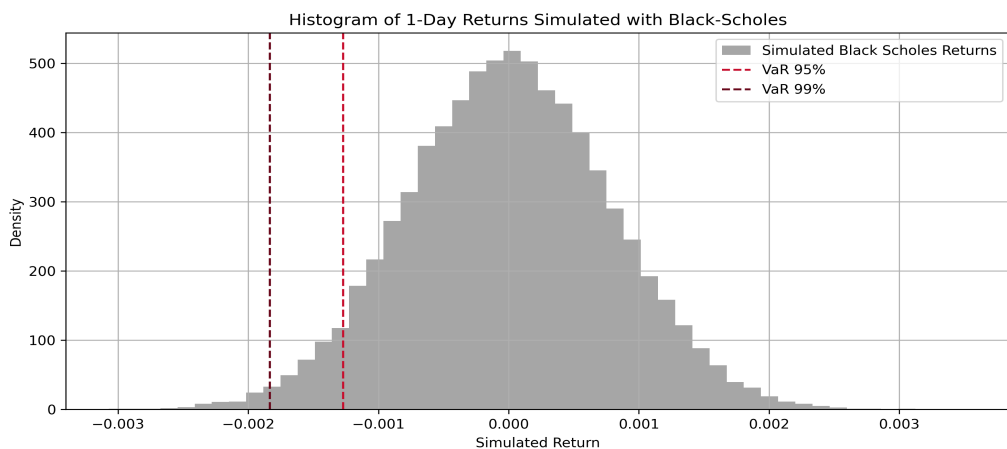


Figure 14: Histogram of 1-day returns simulated using the Black-Scholes model.

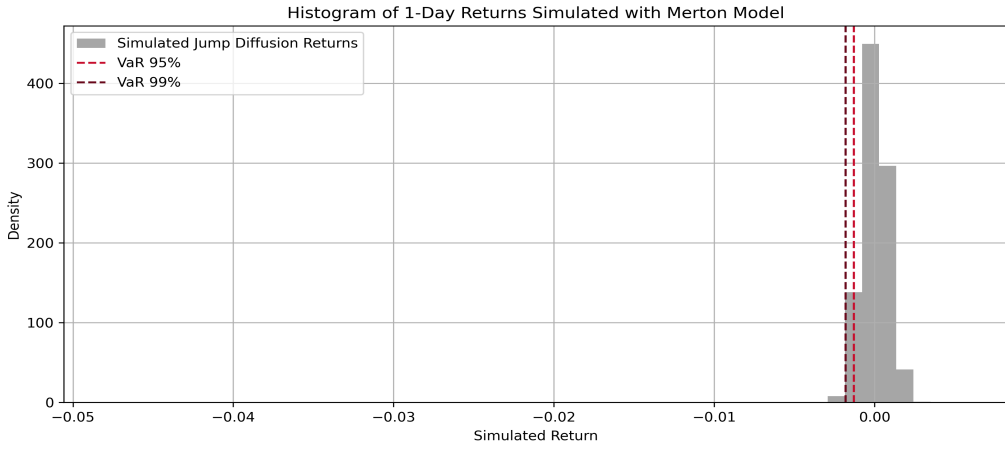


Figure 15: Histogram of 1-day returns simulated using the Merton jump-diffusion model.

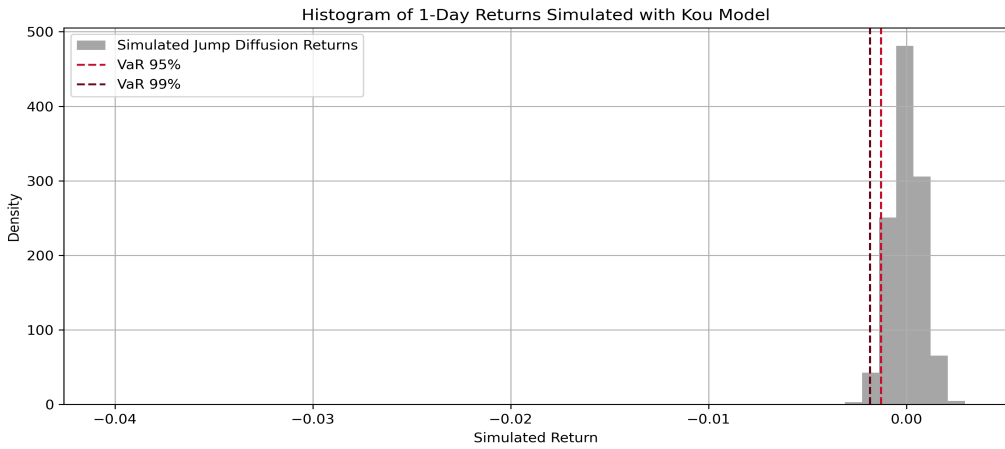


Figure 16: Histogram of 1-day returns simulated using the Kou jump-diffusion model.

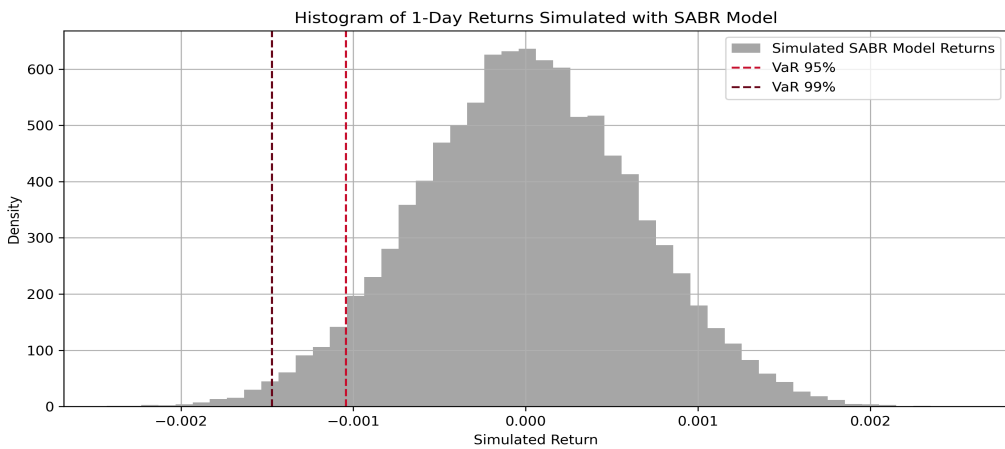


Figure 17: Histogram of 1-day returns simulated using the SABR (Stochastic Alpha Beta Rho) model.

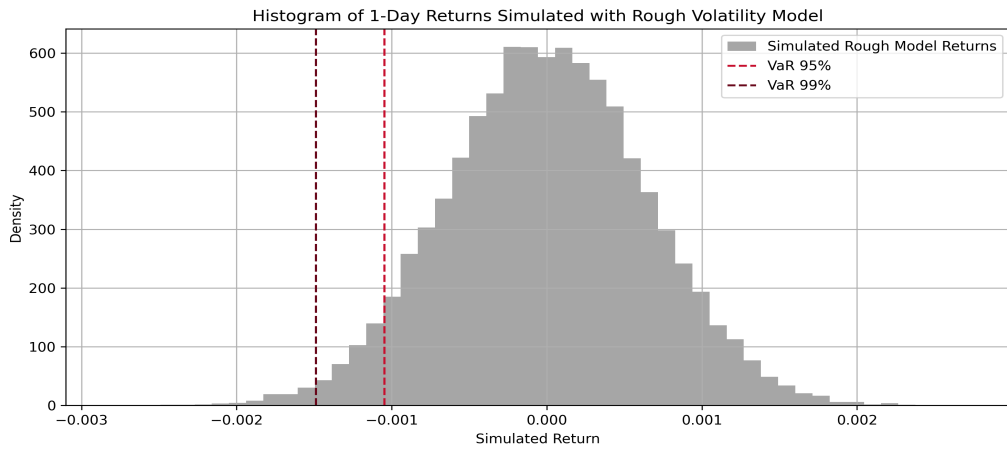


Figure 18: Histogram of 1-day returns simulated using the rough volatility model.

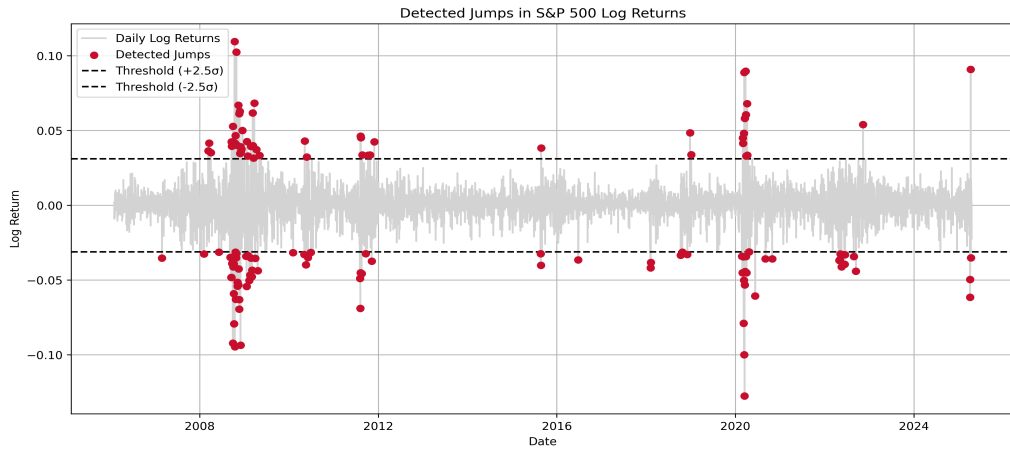


Figure 19: Detected jumps in daily log returns of the S&P 500 index from 2006 to 2024.

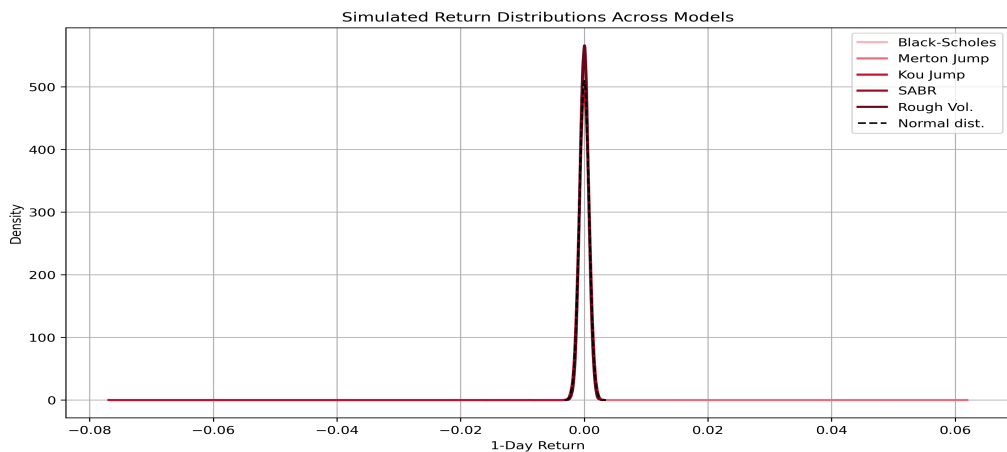


Figure 20: Comparison of simulated 1-day return distributions across models.

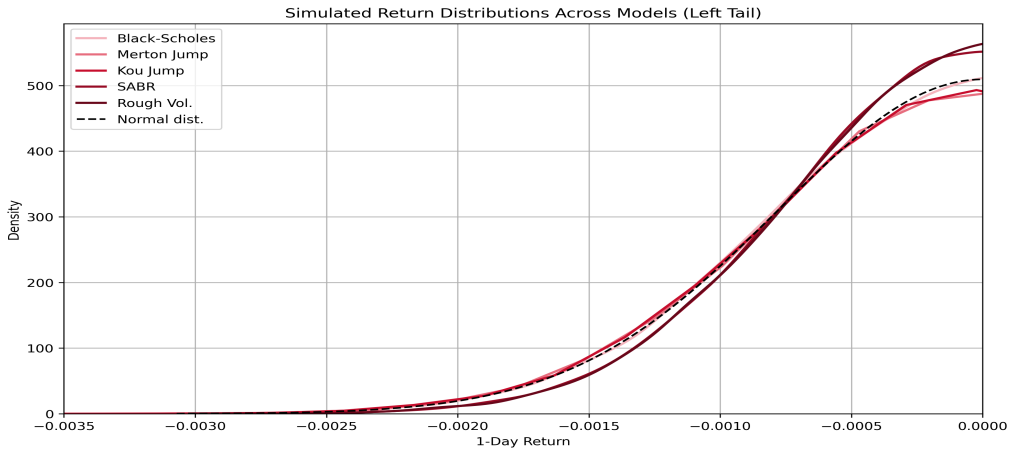


Figure 21: Zoom on the left tail of the simulated 1-day return distributions across models.

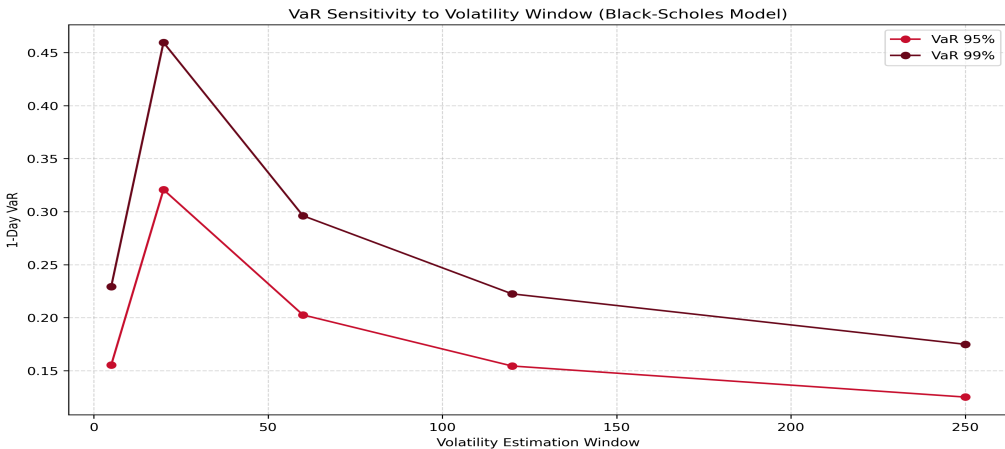


Figure 22: Sensitivity of 1-day Value at Risk (VaR) at the 95% and 99% confidence levels to the length of the rolling volatility window in the Black-Scholes model.

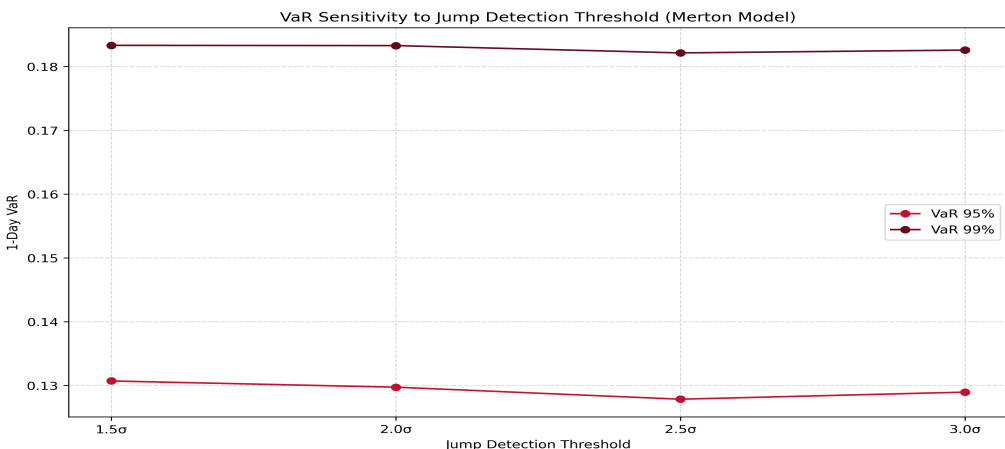


Figure 23: Sensitivity of 1-day Value at Risk (VaR) at the 95% and 99% confidence levels to the jump detection threshold in the Merton jump-diffusion model.

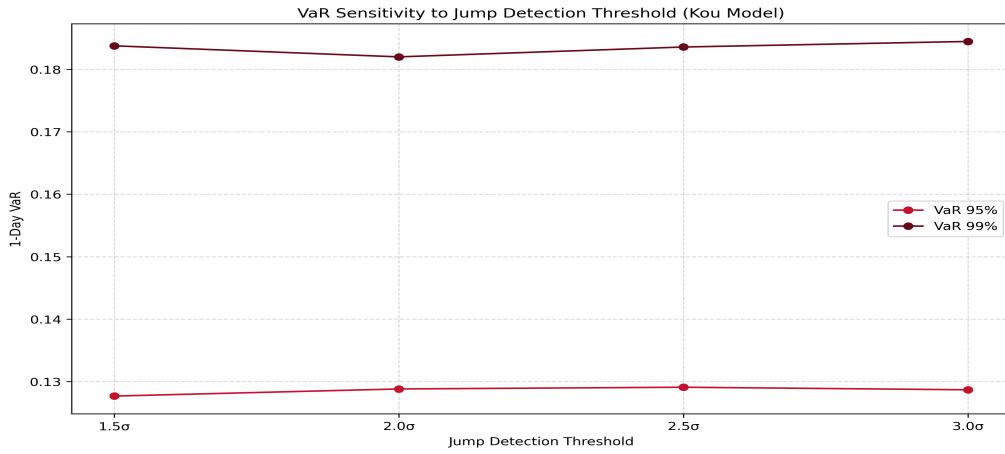


Figure 24: Sensitivity of 1-day Value at Risk (VaR) at the 95% and 99% confidence levels to the jump detection threshold in the Kou jump-diffusion model.

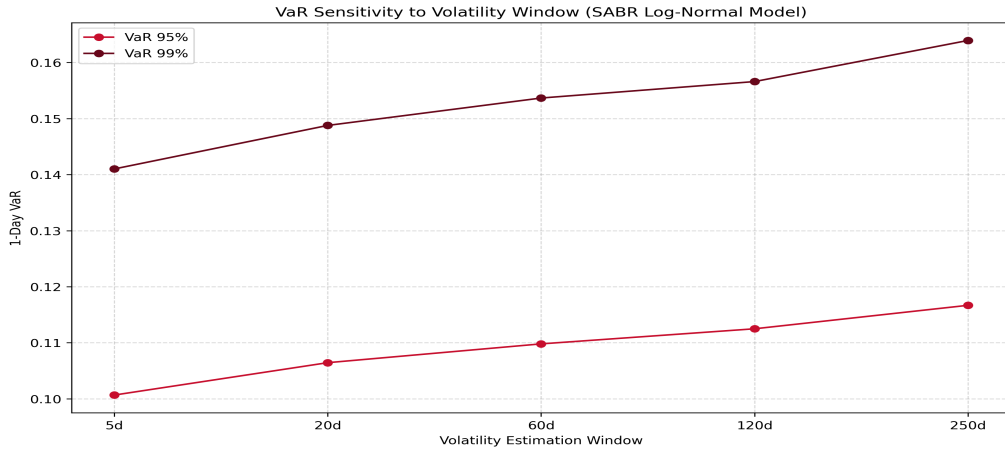


Figure 25: Sensitivity of 1-day Value at Risk (VaR) at the 95% and 99% confidence levels to the volatility estimation window under the SABR log-normal model.

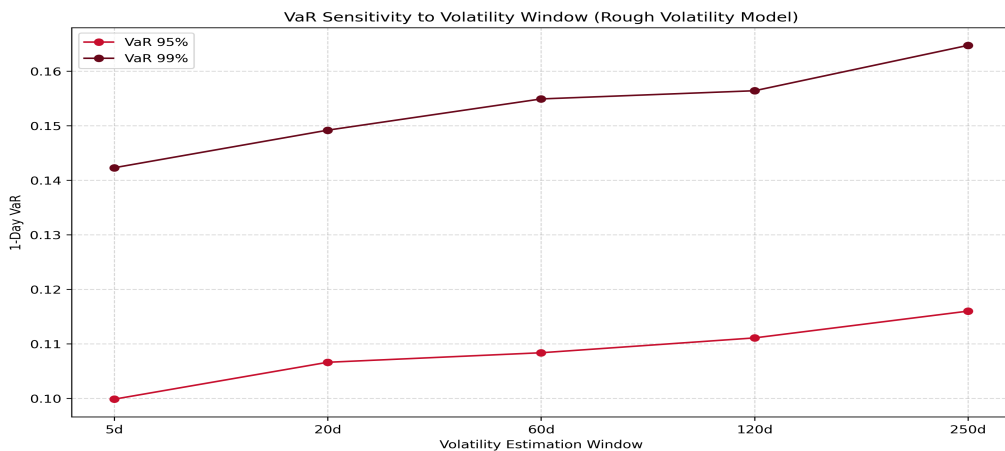


Figure 26: Sensitivity of 1-day Value at Risk (VaR) at the 95% and 99% confidence levels to the volatility estimation window under the rough volatility model.

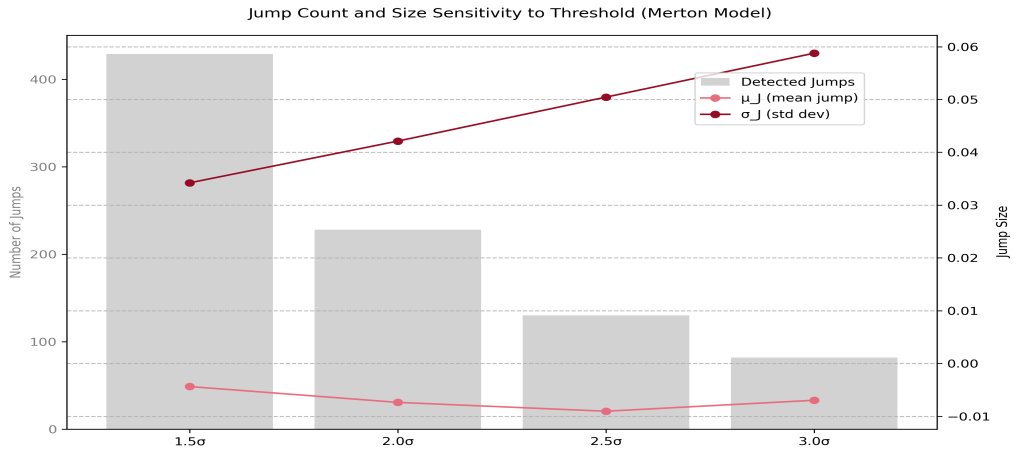


Figure 27: Sensitivity of estimated jump parameters in the Merton model to the detection threshold.

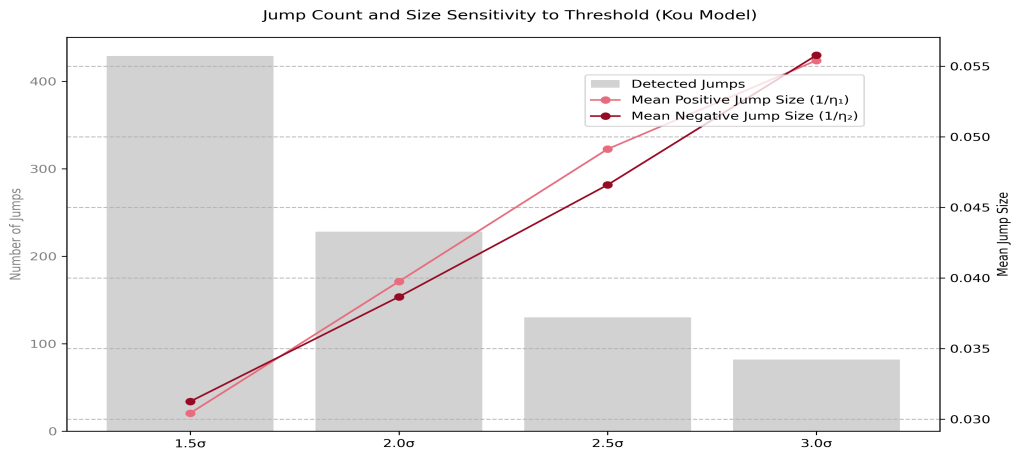


Figure 28: Sensitivity of estimated jump parameters in the Kou model to the detection threshold.

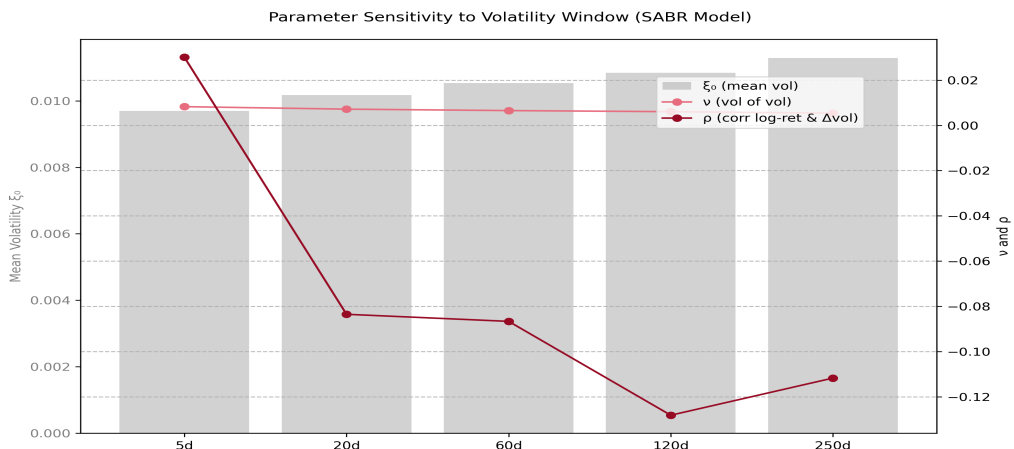


Figure 29: Sensitivity of SABR model parameters to the volatility estimation window.

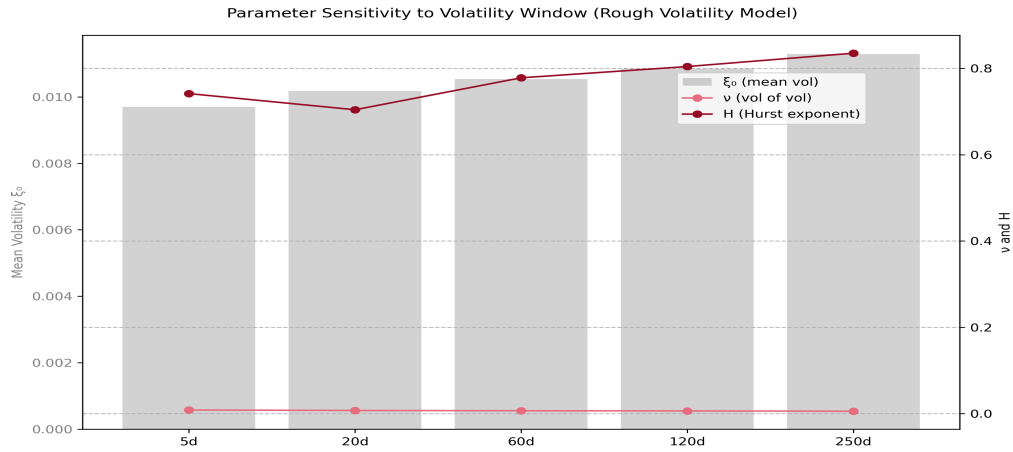


Figure 30: Sensitivity of rough volatility model parameters to the volatility estimation window.

Appendix C

Tables

| Parameter | Value | Description |
|----------------|--------|--------------------------------------|
| μ | 0.0003 | Mean of returns |
| σ | 0.0124 | Standard deviation of returns |
| VaR 95% | 0.1270 | 1-day Value at Risk (95% confidence) |
| VaR 99% | 0.1834 | 1-day Value at Risk (99% confidence) |

Table 2: Estimated parameters and simulated 1-day Value at Risk using Black-Scholes.

| Parameter | Value | Description |
|-----------------------|------------|--------------------------------------|
| λ | 0.0269 | Jumps per day |
| μ_J | -0.0090 | Average jump size |
| σ_J | 0.0505 | Std. dev. of jumps |
| Detected jumps | 130 / 4834 | Total jumps in dataset |
| VaR 95% | 0.1291 | 1-day Value at Risk (95% confidence) |
| VaR 99% | 0.1810 | 1-day Value at Risk (99% confidence) |

Table 3: Estimated parameters and simulated 1-day VaR using the Merton Jump Diffusion model.

| Parameter | Value | Description |
|----------------|--------|--------------------------------------|
| p | 0.3923 | Probability of positive jump |
| η_1 | 20.35 | Positive jump intensity |
| η_2 | 21.46 | Negative jump intensity |
| VaR 95% | 0.1286 | 1-day Value at Risk (95% confidence) |
| VaR 99% | 0.1839 | 1-day Value at Risk (99% confidence) |

Table 4: Estimated parameters and simulated 1-day VaR using the Kou Jump Diffusion model.

| Parameter | Value | Description |
|----------------|---------|--|
| μ | 0.0003 | Annualized drift |
| ξ_0 | 0.0102 | Mean volatility |
| ν | 0.0072 | Volatility of volatility |
| β | 1 | Elasticity parameter |
| ρ | -0.0835 | Correlation between asset and volatility |
| VaR 95% | 0.1043 | 1-day Value at Risk (95% confidence) |
| VaR 99% | 0.1472 | 1-day Value at Risk (99% confidence) |

Table 5: Estimated parameters and simulated 1-day VaR using the SABR model.

| Parameter | Value | Description |
|----------------|--------|--------------------------------------|
| μ | 0.0003 | Annualized drift |
| ξ_0 | 0.0102 | Mean volatility |
| ν | 0.0072 | Volatility of volatility |
| H | 0.7041 | Hurst exponent |
| VaR 95% | 0.1046 | 1-day Value at Risk (95% confidence) |
| VaR 99% | 0.1489 | 1-day Value at Risk (99% confidence) |

Table 6: Estimated parameters and simulated 1-day VaR using the Rough Volatility model.

| Model | VaR 95% | VaR 99% | Kurtosis |
|------------------------------|---------|---------|----------|
| Black-Scholes | 0.1270 | 0.1834 | 3.01 |
| Merton Jump Diffusion | 0.1291 | 0.1810 | 362.93 |
| Kou Jump Diffusion | 0.1286 | 0.1839 | 228.23 |
| SABR Model | 0.1046 | 0.1489 | 3.01 |
| Rough Volatility | 0.1043 | 0.1472 | 2.96 |

Table 7: Comparison of 1-day VaR (95% and 99%) and kurtosis across different volatility models.

| Rolling Window (days) | σ (Realized Volatility) | VaR 95% (Hist.) | VaR 99% (Hist.) |
|-----------------------|--------------------------------|-----------------|-----------------|
| 5 | 0.0150 | 0.1553 | 0.2293 |
| 20 | 0.0304 | 0.3207 | 0.4595 |
| 60 | 0.0193 | 0.2026 | 0.2961 |
| 120 | 0.0149 | 0.1544 | 0.2224 |
| 250 | 0.0120 | 0.1251 | 0.1749 |

Table 8: Sensitivity analysis of the parametric volatility model to the rolling window size used for realized volatility estimation.

| Threshold | Detected Jumps | λ (jumps/-day) | μ_J | σ_J | VaR 95% | VaR 99% |
|-------------------------------|----------------|------------------------|---------|------------|---------|---------|
| 1.5σ | 429 | 0.0887 | -0.0044 | 0.0342 | 0.1307 | 0.1833 |
| 2.0σ | 228 | 0.0472 | -0.0074 | 0.0421 | 0.1297 | 0.1833 |
| 2.5σ | 130 | 0.0269 | -0.0090 | 0.0505 | 0.1278 | 0.1821 |
| 3.0σ | 82 | 0.0170 | -0.0070 | 0.0588 | 0.1290 | 0.1826 |

Table 9: Sensitivity analysis of the Merton Jump Diffusion model to jump detection thresholds.

| Threshold | Detected Jumps | λ (jumps/s/day) | p | η_1 (pos. intensity) | η_2 (neg. intensity) | VaR 95% | VaR 99% |
|-------------------------------|----------------|-------------------------|--------|---------------------------|---------------------------|---------|---------|
| 1.5σ | 429 | 0.0887 | 0.4359 | 32.88 | 32.01 | 0.1277 | 0.1838 |
| 2.0σ | 228 | 0.0472 | 0.3991 | 25.16 | 25.87 | 0.1288 | 0.1820 |
| 2.5σ | 130 | 0.0269 | 0.3923 | 20.35 | 21.46 | 0.1291 | 0.1836 |
| 3.0σ | 82 | 0.0170 | 0.4390 | 18.05 | 17.93 | 0.1287 | 0.1845 |

Table 10: Sensitivity analysis of the Kou Jump Diffusion model to the threshold used for jump detection.

| Volatility Window | ξ_0 (mean vol) | ν (vol of vol) | ρ | VaR 95% | VaR 99% |
|--------------------------|--------------------|--------------------|---------|---------|---------|
| 5d | 0.0097 | 0.0083 | 0.0302 | 0.1007 | 0.1410 |
| 20d | 0.0102 | 0.0072 | -0.0835 | 0.1064 | 0.1488 |
| 60d | 0.0105 | 0.0065 | -0.0867 | 0.1098 | 0.1537 |
| 120d | 0.0108 | 0.0061 | -0.1282 | 0.1125 | 0.1566 |
| 250d | 0.0113 | 0.0054 | -0.1117 | 0.1167 | 0.1639 |

Table 11: Sensitivity analysis of the SABR model to the window size used for volatility estimation.

| Volatility Window | ξ_0 (mean vol) | ν (vol of vol) | H | VaR 95% | VaR 99% |
|--------------------------|--------------------|--------------------|--------|---------|---------|
| 5d | 0.0097 | 0.0083 | 0.7415 | 0.0998 | 0.1423 |
| 20d | 0.0102 | 0.0072 | 0.7041 | 0.1066 | 0.1492 |
| 60d | 0.0105 | 0.0065 | 0.7781 | 0.1084 | 0.1549 |
| 120d | 0.0108 | 0.0061 | 0.8042 | 0.1111 | 0.1564 |
| 250d | 0.0113 | 0.0054 | 0.8352 | 0.1160 | 0.1647 |

Table 12: Sensitivity analysis of the Rough Volatility model to the window size used for volatility estimation.

| Model | Sensitivity | VaR 95% | VaR 99% | Kurtosis | Parameters |
|-------------------------|-------------|---------|---------|----------|--|
| Black-Scholes | 5 | 0.1553 | 0.2293 | 3.01 | $\sigma = 0.015$ |
| | 20 | 0.3207 | 0.4595 | 3.01 | $\sigma = 0.0304$ |
| | 60 | 0.2026 | 0.2961 | 3.01 | $\sigma = 0.0193$ |
| | 120 | 0.1544 | 0.2224 | 3.01 | $\sigma = 0.0149$ |
| | 250 | 0.1251 | 0.1749 | 3.01 | $\sigma = 0.012$ |
| Merton Jump | 1.5σ | 0.1307 | 0.1833 | 955.68 | $\lambda = 0.0887, \mu_J = -0.0044, \sigma_J = 0.0342$ |
| | 2.0σ | 0.1297 | 0.1833 | 955.68 | $\lambda = 0.0472, \mu_J = -0.0074, \sigma_J = 0.0421$ |
| | 2.5σ | 0.1278 | 0.1821 | 955.68 | $\lambda = 0.0269, \mu_J = -0.0090, \sigma_J = 0.0505$ |
| | 3.0σ | 0.1290 | 0.1826 | 955.68 | $\lambda = 0.0170, \mu_J = -0.0070, \sigma_J = 0.0588$ |
| Kou Jump | 1.5σ | 0.1277 | 0.1837 | 1,728.18 | $\lambda = 0.0887, p = 0.4359, \eta_1 = 32.88, \eta_2 = 32.01$ |
| | 2.0σ | 0.1288 | 0.1820 | 1,728.18 | $\lambda = 0.0472, p = 0.3991, \eta_1 = 25.16, \eta_2 = 25.87$ |
| | 2.5σ | 0.1291 | 0.1836 | 1,728.18 | $\lambda = 0.0269, p = 0.3923, \eta_1 = 20.35, \eta_2 = 21.46$ |
| | 3.0σ | 0.1287 | 0.1845 | 1,728.18 | $\lambda = 0.0170, p = 0.4390, \eta_1 = 18.05, \eta_2 = 17.93$ |
| SABR | 5d | 0.1007 | 0.1410 | 2.96 | $\xi_0 = 0.0097, \nu = 0.0083, \rho = 0.0302$ |
| | 20d | 0.1064 | 0.1488 | 2.96 | $\xi_0 = 0.0102, \nu = 0.0072, \rho = -0.0835$ |
| | 60d | 0.1098 | 0.1537 | 3.05 | $\xi_0 = 0.0105, \nu = 0.0065, \rho = -0.0867$ |
| | 120d | 0.1125 | 0.1566 | 2.96 | $\xi_0 = 0.0108, \nu = 0.0061, \rho = -0.1282$ |
| | 250d | 0.1167 | 0.1639 | 2.96 | $\xi_0 = 0.0113, \nu = 0.0054, \rho = -0.1117$ |
| Rough Volatility | 5d | 0.0998 | 0.1423 | 3.01 | $\xi_0 = 0.0097, \nu = 0.0083, H = 0.7415$ |
| | 20d | 0.1066 | 0.1492 | 3.01 | $\xi_0 = 0.0102, \nu = 0.0072, H = 0.7041$ |
| | 60d | 0.1084 | 0.1549 | 3.01 | $\xi_0 = 0.0105, \nu = 0.0065, H = 0.7781$ |
| | 120d | 0.1111 | 0.1564 | 3.01 | $\xi_0 = 0.0108, \nu = 0.0061, H = 0.8042$ |
| | 250d | 0.1160 | 0.1647 | 3.01 | $\xi_0 = 0.0113, \nu = 0.0054, H = 0.8352$ |

Table 13: Sensitivity analysis across all volatility models with varying calibration inputs.

Appendix D

Mathematical Derivations

We start from the BSM with an added “Jump” component:

$$\frac{dS_t}{S_t} = \mu dt + \sigma dW_t + \text{Jump}$$

This jump component has two sources of randomness: the *arrival*, which is modeled like a Poisson process, and the *magnitude*, which is assumed to follow a log-normal distribution.

The magnitude of a jump $\ln(Y_t) \sim N(\mu, \sigma^2)$ can be thought of as a “scaling factor.”

Right after a jump, the stock price moves to:

$$S_t \rightarrow Y_t S_t,$$

where if $0 < Y_t < 1$, it will be a *negative* jump, and otherwise it will be a *positive* jump

Hence,

$$dS_t = Y_t S_t - S_t \rightarrow \frac{dS_t}{S_t} = Y_t - 1.$$

We can add this to the BS dynamics:

$$\frac{dS_t}{S_t} = \mu dt + \sigma dW_t + (Y_t - 1).$$

Note: for the arrival of the jumps, we assume they follow a Poisson process with parameter λ :

$$dN_t = \begin{cases} 1, & \text{with probability } \lambda dt, \\ 0, & \text{with probability } 1 - \lambda dt. \end{cases}$$

Thus we can update the dynamics:

$$\frac{dS_t}{S_t} = \mu dt + \sigma dW_t + (Y_t - 1) dN_t.$$

We want to know what the “expected” jump will be at any given time, to absorb it into a drift-correction parameter. Note that

$$\mathbb{E}[(Y_t - 1) dN_t] = \mathbb{E}[Y_t - 1] \mathbb{E}[dN_t] = k \lambda dt,$$

where $k = \mathbb{E}[Y_t - 1]$. Thus the jump process introduces an extra “drift,” and we subtract it off for a martingale adjustment:

$$\frac{dS_t}{S_t} = \mu dt + \sigma dW_t + (Y_t - 1) dN_t - \lambda k dt.$$

We must also account for the possibility of multiple jumps at the same instant. If $dN_t = 3$, say, with jump-sizes Y_1, Y_2, Y_3 , then

$$S_t \longrightarrow S_t Y_1 Y_2 Y_3 = S_t \prod_{j=1}^3 Y_j,$$

and in general

$$\frac{dS_t}{S_t} = \mu dt + \sigma dW_t + \left(\prod_{j=1}^{dN_t} Y_j - 1 \right) - \lambda k dt.$$

Putting all terms together in the usual SDE form we obtain our final equation,

$$dS_t = S_t(\mu - \lambda k) dt + \sigma S_t dW_t + S_t \left(\prod_{j=1}^{dN_t} Y_j - 1 \right)$$